Paper

World Atmospheric CO_2, Its ^{14}C Specific Activity, Non-fossil Component, Anthropogenic Fossil Component, and Emissions (1750–2018)

Kenneth Skrable, George Chabot, and Clayton French[1]

Abstract—**After 1750 and the onset of the industrial revolution, the anthropogenic fossil component and the non-fossil component in the total atmospheric CO_2 concentration, *C(t)*, began to increase. Despite the lack of knowledge of these two components, claims that all or most of the increase in *C(t)* since 1800 has been due to the anthropogenic fossil component have continued since they began in 1960 with "Keeling Curve: Increase in CO_2 from burning fossil fuel." Data and plots of annual anthropogenic fossil CO_2 emissions and concentrations, *C(t)*, published by the Energy Information Administration, are expanded in this paper. Additions include annual mean values in 1750 through 2018 of the ^{14}C specific activity, concentrations of the two components, and their changes from values in 1750. The specific activity of ^{14}C in the atmosphere gets reduced by a dilution effect when fossil CO_2, which is devoid of ^{14}C, enters the atmosphere. We have used the results of this effect to quantify the two components. All results covering the period from 1750 through 2018 are listed in a table and plotted in figures.These results negate claims that the increase in *C(t)* since 1800 has been dominated by the increase of the anthropogenic fossil component. We determined that in 2018, atmospheric anthropogenic fossil CO_2 represented 23% of the total emissions since 1750 with the remaining 77% in the exchange reservoirs. Our results show that the percentage of the total CO_2 due to the use of fossil fuels from 1750 to 2018 increased from 0% in 1750 to 12% in 2018, much too low to be the cause of global warming.**
Health Phys. 122(2):291–305; 2022

Key words: ^{14}C; emissions, atmospheric; environs; radiation protection

INTRODUCTION

At an elapsed time of *t* years since 1750 (the start of the industrial revolution with the onset of the use of fossil fuels in vehicles and power plants), atmospheric CO_2 concentrations, *C(t)*, increased along with increases in temperatures. Atmospheric measurements of *C(t)* were not available until 1958 at the Mauna Loa, HI, observatory of the National Oceanic and Atmospheric Administration (NOAA), which has provided the longest record of atmospheric measurements of the total CO_2 initiated by Charles Keeling in 1958 at the Mauna Loa observatory (Keeling 1960). Based on our knowledge, the anthropogenic fossil component, $C_F(t)$, and non-fossil component, $C_{NF}(t)$, in *C(t)* have never been estimated by NOAA at its observatories or at any other observatory from atmospheric measurements of CO_2. Despite the lack of knowledge of the components of *C(t)*, claims have been made in the scientific literature (CSIRO 2014; Rubino et al. 2013, 2019) that all or most of the increase in *C(t)* since 1800 has been due to the anthropogenic fossil component, $C_F(t)$.

Other atmospheric measurements of *C(t)* began in 2003 at the NOAA observatory in Niwot Ridge, including measurements of the three isotopes of carbon: ^{12}C, ^{13}C, and ^{14}C. Carbon-14 is a radioactive isotope of carbon having a half-life of 5,730 y. Carbon-14 atoms are produced in the atmosphere by interactions of cosmic rays, and they have reached an essentially constant steady state activity, i.e., disintegration rate, in the total world environment (Eisenbud and Gesell 1997). The age of fossil fuels is much longer than the 5,730 y half-life of the ^{14}C radioactive isotope; consequently, fossil fuels are devoid of the ^{14}C isotope. When the anthropogenic fossil component of CO_2 is released to the atmosphere, the specific activity of ^{14}C, *S(t)* in *C(t)*, decreases. The units of *S(t)* used in this paper are disintegrations per minute per gram of carbon abbreviated as dpm $(gC)^{-1}$, the common units used in ^{14}C dating. The ratio R_{S13} of the ($^{13}C/^{12}C$) atoms and the ratio R_{S14} of the ($^{14}C/^{12}C$) atoms at the Niwot Ridge observatory are used to calculate two statistics designated respectively in this paper as *d13C* and *D14C*, both of which are said to decrease when the anthropogenic fossil component, $C_F(t)$, increases in the atmosphere. As discussed later in Table 1, values of the annual mean specific activity, *S(t)*, are calculated in this paper from annual mean values of the *D14C* statistic.

Both the *d13C* and *D14C* statistics represent 1,000 times the relative deviations of their respective ($^{13}C/^{12}C$)

[1]University of Massachusetts Lowell, 1 University Avenue, Lowell, MA 01854.

The authors declare no conflicts of interest.

For correspondence contact Kenneth Skrable via email at **skrablekw@aol.com**.

(*Manuscript accepted* 22 *July* 2021)

Supplemental digital content is available in the HTML and PDF versions of this article on the journal's website www.health-physics.com.

0017-9078/21/0

DOI: 10.1097/HP.0000000000001485

and (^{14}C /^{12}C) atom ratios from those of a 1950 standard (Karlen et al. 1964) when expressed in per mil, given by the symbol ‰. This magnification increases their underlying relative deviations and slopes in plots by a factor 1,000. While such amplification techniques often are useful for displaying very small changes in quantities of interest, the interpretation of such magnified changes must be attended with some care. In the cases of concern here, the resultant steep slopes in plots likely have led persons throughout the world to conclude that the anthropogenic component has dominated the increase of CO_2 and caused global warming. We believe that both statistics have been misused to validate the anthropogenic fossil component, $C_F(t)$, as the major cause of the increase of $C(t)$.

Global carbon cycle and its effect on CO_2 quantities

The global carbon cycle for CO_2 is described by the Energy Information Administration (EIA 2020). Natural, two-way exchanges of CO_2 occur between the atmosphere and its two exchange reservoirs, the oceans and terrestrial biosphere. Two-way exchanges with the atmosphere also occur from changes in land use. The ocean is the largest reservoir of CO_2, and it contains 50 times that for the atmosphere and 19 times that for the terrestrial biosphere (Water Encyclopedia 2005). All of the two way exchanges are considered in this paper to be comprised of both the non-fossil component and the anthropogenic fossil component. Annual changes, $DC_{NF}(t)$ in $C_{NF}(t)$, in the atmosphere relative to the 1750 initial value, $C(0)$, can be positive or negative depending on the net flow of CO_2 between the atmosphere and its exchange reservoirs as well as on land use changes. A one-way pathway of anthropogenic fossil CO_2 into the atmosphere from fossil fuel combustion and industrial fuel processes since 1750 is represented by annual emissions, $DE(t)$, of anthropogenic fossil CO_2 to the atmosphere, which have been increasing each year since 1750. These emissions over time t result in increasing annual mean anthropogenic fossil concentrations, $C_F(t)$, that result in specific activities, $S(t)$, of ^{14}C in $C(t)$ that are increasingly lower than the initial value, $S(0)$. This dilution of $S(0)$ in $C(0)$ in 1750 by the presence of $C_F(t)$ in $C(t)$ corresponds to what is described as the Suess effect (Suess et al. 1967).

Use of symbols, equations, and significant digital content

In this paper, it is important for the reader to be aware of the following use of symbols, equations, and supplemental digital content (SDC), http://links.lww.com/HP/A210. All symbols for quantities in equations and the text are italicized. Symbols for expected values of a CO_2 quantity calculated from an analytical equation are shown in brackets, < >; for example, expected specific activity, $<S(t)>$, and expected anthropogenic fossil component, $<C_F(t)>$, which is calculated from the value of $<S(t)>$. Other CO_2 quantities are considered as random variables either estimated directly from measurements or calculated from other measured CO_2 quantities. The standard use of sequential numbers in the text for equations is not employed. Equations used to calculate a quantity in a numbered column of a table have that number, but equations listed below a table are not numbered. Equations and their numbers are listed in the figures. Definitions for all symbols used in this paper are listed in the Appendix. Table 2 (http://links.lww.com/HP/A210) contains 8 pages of significant digital content of the values of CO_2 quantities in 1750 through 2018 (Skrable et al. 2021). Table 2a contains a partial listing of the data in Table 2. All of the values for CO_2 quantities in Table 2 are plotted in the figures.

Glacial–interglacial cycles

A NOAA link[3] gives a description and (Fig. 1) of glacial-interglacial cycles from 350,000 y ago to the present. Present in the figure is defined as 1950 AD, the convention used in radiocarbon dating because H-bomb testing in the 1950s distorted radiocarbon ages in many materials (personal communication, Bauer 2021[2]).

The cause of glacial-interglacial cycles in the figure is stated to be due to variations in Earth's orbit through time, which changes the amount of solar radiation received by Earth. The figure includes three plots from the top to the bottom of the figure: (1) July insolation at 65° N (Wm^{-2}), (2) temperature change from present (°C), and (3) atmospheric CO_2 (ppm). The caption in the figure describes its content. It also is stated in the article: "The most recent glacial period occurred between about 120,000 and 11,500 years ago. Since then, Earth has been in an interglacial period called the Holocene."

During the last long glacial period, the oceans absorbed a large amount of CO_2 from the atmosphere. It appears in the figure that Earth is still in the Holocene interglacial period that started 11,500 y ago. Its peak temperature change over the 11,500 years, thus far in 1950, appears to be significantly less than those over the three previous interglacial periods. Its peak CO_2 appears less than 300 ppm and less than the peak value in the previous interglacial period. Thus, the increase in CO_2 that Earth has been experiencing since 1800 appears to have started more than 5,000 years ago.

Increase in $^{14}CO_2$ from high altitude nuclear bomb tests

A Wikipedia link[4] for ^{14}C describes the increase in the concentration of $^{14}CO_2$ in the atmosphere that resulted from high altitude nuclear bomb tests, circa 1955–1963. Based on the figure in the Wikipedia link, $^{14}CO_2$ from the atmospheric bomb tests during this period would be significant in 1955 to about 2005. For the purpose of estimating the

[2]Personal communication, Bauer BA, National Centers for Environmental Information, NOAA, 154 Patton Ave., Federal Bld., Washington, DC, 15 March 2021.
[3]https://www.ncdc.noaa.gov/abrupt-climate-change/Glacial-Interglacial%20Cycles, Accessed 26 October 2021.
[4]Wikipedia. http://en.wikipedia.org/wiki/Carbon-14. Accessed 12 October 2021.

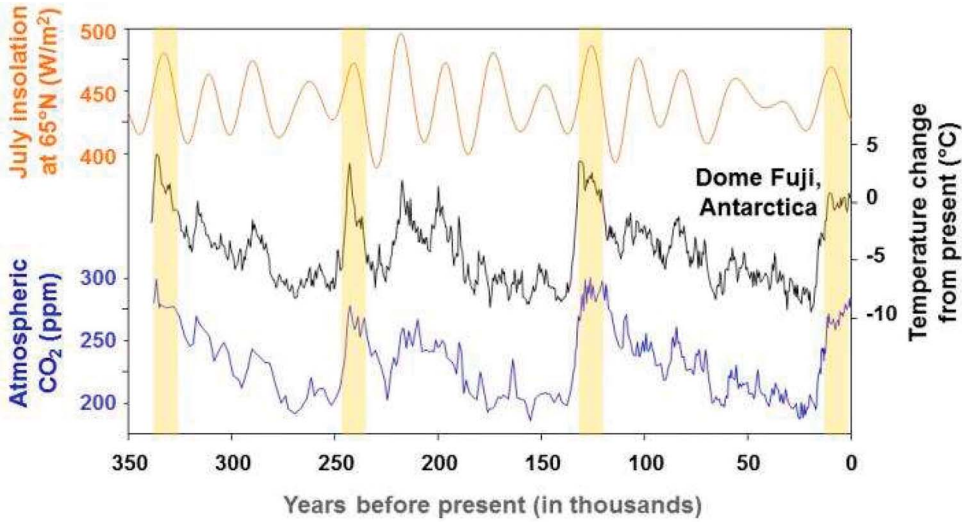

Fig. 1. Glacial-interglacial cycles. Solar radiation varies smoothly through time (top, orange line) with a strong cyclicity of ~23,000 years, as seen in this time series of July incoming solar radiation at 65°N (Berger and Loutre 1991). In contrast, glacial–interglacial cycles last ~100,000 years (middle, black line) and consist of stepwise cooling events followed by rapid warmings, as seen in this time series inferred from hydrogen isotopes in the Dome Fuji ice core from Antarctica (Kawamura et al. 2007). Atmospheric CO_2 measured from bubbles in Dome Fuji ice (bottom, blue line) shows the same pattern as the temperature time series (Kawamura et al. 2007). Yellow columns indicate interglacial periods.

anthropogenic fossil and non-fossil components of CO_2, measurements of ^{14}C specific activities of atmospheric CO_2 during this period should be corrected for the contribution from bomb tests. Outside of this period, no correction would be required. The Wikipedia link gives the world inventory of ^{14}C:

- Global inventory: ~8500 PBq (about 50 tonnes):
- Atmosphere: 140 PBq (840 kg);
- From nuclear testing (till 1990): 220 PBq (1.3 tonnes); and
- Terrestrial materials: the balance.

Thus, the portion of $^{14}CO_2$ from nuclear testing is about 2.6% of the global inventory, which now is mostly in the ocean reservoir. Some part of this 2.6% is expected to be released to the atmosphere, opposing the dilution effect from burned fossil fuels, although it is expected to be small in comparison to the dilution effect of fossil fuel CO_2.

A NOAA link[5] about the bomb spike provides a plot of the *D14C* statistic, and the following statement is made: "By the 1980s, most of the "bomb" ^{14}C had been absorbed into the oceans and land biota, leaving slightly elevated levels in the atmosphere. Yet atmospheric ^{14}C levels continue to decrease–now because of fossil fuel CO_2 emissions."

In this paper, we calculate annual mean specific activities, *S(t)*, from annual mean values of the *D14C* statistic in 2004 through 2012, which are calculated from data obtained from NOAA (Lehman and Miller 2019). These *S(t)* values along with our chosen value, *S(0)*, in 1750 then are used in Table 1 to estimate expected specific activities, $<S(t)>$, in 1750 through 2018 from an approximation fitting function. Therefore, the $<S(t)>$ values in this paper are not expected to be influenced significantly by $^{14}CO_2$ from nuclear bomb tests.

MATERIALS AND METHODS

The calculation of the annual mean CO_2 components, $C_F(t)$ and $C_{NF}(t)$, requires starting with estimates of the values present in 1750 ($t = 0$). The time t is calculated in years from 1750 to the year of the annual mean values of the CO_2 components; for example, $t = 1$ y in 1751 and 200 y in 1950. The annual mean total concentrations, *C(t)*, along with their ^{14}C specific activities, *S(t)*, present in the atmosphere at time t years after 1750, are evaluated in this paper as follows. In each year, the values of *C(t)* and *S(t)* are compared to the initial value, *C(0)*, and its specific activity, *S(0)*, of ^{14}C present in 1750. The value of *C(0)* is assumed to be comprised of an unspecified natural background fossil component and natural non-fossil CO_2. The value of *C(0)* also is treated in our analysis as the initial, natural, non-anthropogenic fossil component, $C_{NF}(0)$. The comparisons yield estimates of the annual mean values of the *anthropogenic fossil* (F) component, $C_F(t)$, and the *non-fossil* (NF) component, $C_{NF}(t)$, present in *C(t)* each year. The two components are calculated from simple equations that account for the change, $DC_{NF}(t)$, each year in the non-fossil component, which results from the redistribution of all CO_2 among its reservoirs, including the atmosphere, oceans, and terrestrial biosphere as well as from changes in land use. The sum of *C(0)* and $DC_{NF}(t)$ equals the non-fossil component, $C_{NF}(t)$, present in the atmosphere at time t years after 1750.

[5]https://www.esrl.noaa.gov/gmd/outreach/isotopes/bombspike.html. Accessed 26 October 2021

Table 1. Niwot Ridge, Colorado annual mean specific activity, *S(t)*, and expected specific activity, <*S(t)*>, of ^{14}C in *C(t)* in 1750 through 2018.[a]

Year	Time, *t*, Since 1750 (years)	*D14C* (‰)	^{14}C Decay Factor F_d	*d13C* (‰)	^{13}C Fraction. Factor F_{13}	R_{S13} (13C/12C)	R_{S14} (14C/12C)	(1) *S(t)* Specific Activity [dpm $(gC)^{-1}$]	(2) <*S(t)*> Specific Activity [dpm $(gC)^{-1}$]
1750*	0	–	–	−6.50	0.9631	0.00000	–	16.33	16.33
1775	25	–	–	–	–	–	–	–	16.32
1800	50	–	–	–	–	–	–	–	16.31
1850	100	–	–	–	–	–	–	–	16.28
1900	150	–	–	–	–	–	–	–	16.25
1950	200	–	–	–	–	–	–	–	16.10
1975	225	–	–	–	–	–	–	–	15.80
2000	250	–	–	–	–	–	–	–	15.06
2004	254	64.61	0.9935	–8.348	0.9667	0.01114	1.304×10^{-12}	14.87	14.87
2005	255	58.21	0.9934	–8.245	0.9665	0.01114	1.296×10^{-12}	14.78	14.81
2006	256	55.57	0.9932	–8.311	0.9666	0.01114	1.293×10^{-12}	14.74	14.76
2007	257	50.91	0.9931	–8.294	0.9666	0.01114	1.287×10^{-12}	14.68	14.71
2008	258	46.93	0.9930	–8.321	0.9666	0.01114	1.283×10^{-12}	14.63	14.65
2009	259	43.22	0.9929	–8.324	0.9667	0.01114	1.278×10^{-12}	14.58	14.59
2010	260	38.88	0.9928	–8.369	0.9667	0.01114	1.273×10^{-12}	14.52	14.53
2011	261	33.77	0.9926	–8.415	0.9668	0.01114	1.267×10^{-12}	14.45	14.47
2012	262	29.99	0.9925	–8.425	0.9668	0.01114	1.262×10^{-12}	14.39	14.40
2018**	268	4.734	0.9918	–8.573	0.9671	0.01114	1.232×10^{-12}	14.05	13.96
	Relative % Change =	−92.67	−0.17	2.70	0.05	−0.02	−5.51	−5.51	−6.07

[a]Constants and equations:

$R_{std13} \equiv (^{13}C/^{12}C)$ ratio = 0.011237 in 1950. $R_{std14} \equiv (^{14}C/^{12}C)$ ratio = 1.176×10^{-12} in 1950.

$k = 1.1404 \times 10^{13}$ dpm $(gC)^{-1}$ per unit $(^{14}C/^{12}C)$ ratio.

$F_d = e^{\lambda(200\,-\,t)}$, for t years after 1750 and $\lambda = \ln 2\ (5{,}730\ y)^{-1}$. $F_{13} = [0.975(1 + 0.001\ d13C)^{-1}]^2$.

$R_{S13} = (1 + 0.001\ d13C)R_{std13}$. $R_{S14} = (1 + 0.001\ D14C)\ R_{std14}(F_d\ F_{13})^{-1}$.

S(t) ≡ annual mean specific activity = $k\ R_{S14}$ in units of dpm $(gC)^{-1}$.

$S_{std14} \equiv$ standard specific activity = $k\ R_{std14}$ = 13.41 dpm $(gC)^{-1}$ in 1950.

<*S(t)*> ≡ expected specific activity of C(t) calculated from Equation (2) for the approximation fitting function, dpm $(gC)^{-1} = 16.33\text{-}(10^{-22.82})\ t^{9.542}\text{–}0.00049\ t$.

Although the initial value, *C(0)*, in 1750 has a background fossil component, such as emissions from volcanos, it is small in comparison to the anthropogenic fossil component (Gerlach 2011), and this natural background fossil component is not considered directly in the derivation of the equation for $C_F(t)$. Because the anthropogenic fossil component, $C_F(t)$, is assumed to be zero in 1750, the change, $DC_F(t)$, in the anthropogenic fossil component in the atmosphere in any year since 1750 is identical to the concentration, $C_F(t)$, present in that year. The specific activity, *S(t)* of *C(t)*, resulting from the presence of $C_F(t)$ at time *t* has the same value calculated from the dilution of the initial specific activity, *S(0)* in *C(0)*, in 1750 by the presence of $C_F(t)$ in *C(t)* at time *t*. Changes, $DC_F(t)$ and $DC_{NF}(t)$ are independent processes that automatically incorporate any redistribution of CO_2 in its reservoirs and changes in land use. Thus, *C(t)* can be expressed: $C(t) = DC_F(t) + DC_{NF}(t) + C(0)$. The value of $DC_F(t)$ varies each year only with the annual mean specific activity, *S(t)* in *C(t)*, in units of dpm $(gC)^{-1}$. The value of $DC_{NF}(t)$ that occurs each year depends only on the change in the ^{14}C activity per unit volume of the atmosphere in units, for example, of dpm m^{-3}.

Equations used to calculate the values of the *d13C* and *D14C* statistics reported by NOAA

Annual mean values of the *d13C* and *D14C* statistics are expressed in the common unit of per mil represented by the symbol ‰. Values of both statistics are used in plots by NOAA and others to depict time trends in the anthropogenic fossil component. The NOAA *d13C* data (White et al. 2015) are used to calculate the annual mean *d13C* values listed in Table 1 along with applicable equations and constants listed below the table and discussed here. The NOAA data of *D14C* (Lehman and Miller 2019) are used to calculate the annual mean *D14C* values listed in Table 1, which are used to estimate the annual mean *S(t)* values in *C(t)* in 2004 through 2012. Equations for both statistics are given at the NOAA website at a link[6] for "Determining Delta Values" and at a link[7] for "The Data: The Story Told from CO_2 Samples" (NOAA).

Values of the *d13C* statistic are obtained by an equation containing the $(^{13}C/^{12}C)$ atom ratios, R_{S13} in *C(t)*, for a sample, and the ratio, R_{std13}, for a 1950 standard:

$$d13C = \left(\frac{\left(\frac{13C}{12C}\right)_{sample}}{\left(\frac{13C}{12C}\right)_{standard}} - 1\right) 1,000‰$$

$$= \left(\frac{R_{S13}}{R_{std13}} - 1\right) 1,000‰$$

$$= \left(\frac{R_{S13} - R_{std13}}{R_{std13}}\right) 1,000‰.$$

As indicated by the last equality, the reported value of the *d13C* statistic is actually a relative delta value multiplied by 1,000‰ and not simply the measured annual mean ratio, R_{S13}, of $(^{13}C/^{12}C)$ atoms in *C(t)* as sometimes inferred incorrectly in the literature (CSIRO 2014). It also should be noted for the quantities shown in the second equality that the *d13C* statistic is a linear function of R_{S13} whose intercept of −1 and slope of $(R_{std13})^{-1}$ are multiplied by 1,000‰.

The annual mean ratios, R_{S13}, of $(^{13}C/^{12}C)$ atoms in *C(t)* listed in Table 1 are calculated by the equation for *d13C* above rearranged: $R_{S13} = (1 + 0.001\ d13C)\ R_{std13}$, which is listed below Table 1. All values in 2004 and afterward have the same value of 0.01114, which is slightly smaller than that of the 1950 standard ratio, R_{std13}, of 0.011237. Thus, it appears that changes in the *d13C* values from 2004 to 2018 reflect very small changes in the ratios, R_{S13}, of $(^{13}C/^{12}C)$ atoms in *C(t)*. The slope of a plot of R_{S13} versus *d13C* values is 0.001 R_{std13}, which equals (0.001)(0.011237) or 0.000011237 per ‰ of *d13C*, which explains why the ratio, R_{S13}, is insensitive to even large changes in the *d13C* statistic.

Much of the discussion above for *d13C* and R_{S13} applies to *D14C* and R_{S14}. The factor F_d in Table 1 is added to the equation for *d13C* to account for the decay of ^{14}C atoms from the year of the annual mean value for *C(t)* and its *D14C* statistic to the year 1950 for the standard. The factor F_{13} in Table 1 is added to account for the fractionation of ^{13}C atoms relative to that of the 1950 standard, which has an assigned *d13C* value of −25‰ (Miller et al. 2013). Equations for these two factors are listed below Table 1. The equation revised from that for *d13C* yields the annual mean value of the *D14C* statistic calculated from data provided by NOAA:

$$D14C = \left(\frac{R_{S14}F_dF_{13}}{R_{std14}} - 1\right) 1,000‰$$

$$= \left(\frac{S(t)F_dF_{13}}{S_{std14}} - 1\right) 1,000‰$$

$$= \left(\frac{R_{S14}F_dF_{13} - R_{std14}}{R_{std14}}\right) 1,000‰$$

The latter equality shows that the *D14C* statistic also is a relative delta value multiplied by 1,000‰. The second equality is expressed in terms of the specific activities *S(t)*

[6]https://www.esrl.noaa.gov/gmd/outreach/isotopes/deltavalues.html. Accessed 26 October 2021
[7]https://www.esrl.noaa.gov/gmd/outreach/isotopes/mixing.html. Accessed 26 October 2021

and S_{std14} calculated from the respective products of their ratios, R_{S14} and R_{std14}, and the conversion constant k listed below Table 1. The factors F_d and F_{13} in Table 1 change very little from 2004 to 2012, and the first expression for *D14C* is approximated by a general linear equation of *D14C* versus R_{S14} multiplied by 1,000‰: $y \approx (A\ x + B)$ 1,000‰, where y is *D14C*; A is $[F_d F_{13}(R_{std14})^{-1}]$, which approximates the slope of the linear equation before multiplying by 1,000‰; x is R_{S14}; and B is −1 and the y intercept of the underlying linear equation. Thus, a plot of values of the *D14C* statistic versus R_{S14}, when expressed in per mil (‰), has the slope A and the y intercept, −1, both multiplied by a factor of 1,000 in this underlying linear equation. The values of R_{S14} and *S(t)* for anthropogenic fossil CO_2 are zero; therefore, its *D14C* value is −1,000‰. Annual mean *D14C* values for all applicable air sampling events in each year for the Niwot Ridge site are used in this paper to calculate the annual mean ratios, R_{S14}, of ($^{14}C/^{12}C$) atoms. Annual mean ratios, R_{S14}, of ($^{14}C/^{12}C$) atoms in *C(t)* listed in Table 1 are calculated by rearrangement of the equation for *D14C*: $R_{S14} = (1 + 0.001\ D14C)\ R_{std14}\ (F_d\ F_{13})^{-1}$, which is listed below Table 1. It is noted that R_{S14} is the annual mean value in *C(t)* and in *D14C* in the year of the measurement and not the year 1950 for the standard ratio, R_{std14}. Thus, the measured value of R_{S14} is independent of all three factors to the right of the bracketed expression for R_{S14}, as well as the value for the *d13C* statistic in the equation for the F_{13} factor listed below Table 1. Values of R_{S14} and R_{std14} listed in Table 1 are multiplied by the constant factor k listed below Table 1 to obtain their listed respective specific activities *S(t)* and S_{std14}. The value for the factor k is 1.1404×10^{13} dpm $(gC)^{-1}$ per unit ($^{14}C/^{12}C$) atom ratio. It is calculated from the reported half-life of 5,730 y for ^{14}C, a constant percent ^{12}C abundance of 98.897, and a constant atomic weight of carbon of 12.0111 g $mole^{-1}$. The values of the latter two quantities in 2004 through 2012 vary slightly in their sixth significant digit because of a very slight decrease in the R_{S13} ratio. These very small changes have no practical significance on the results in this paper, which apply to an essentially constant value of the factor k from 1750 through 2020.

Process used to obtain expected specific activities, <*S(t)*>, in 1750 through 2018

NOAA has provided limited *D14C* data for the Niwot Ridge, CO, observatory beginning in 2004 and ending in 2012; these data have been used in this paper to calculate nine annual mean input specific activities, *S(t)*, in Table 1. Despite the fact that the *D14C* program has continued, we have been unable to obtain from NOAA the data for 2013 through 2020. To make up for the limited *D14C* data, a process is used to estimate expected specific activities, <*S(t)*>, from an approximation fitting function applicable to the years 1750 through 2018. The process used to estimate the parameter values for the approximation fitting function is described as follows.

The solid trend line in Fig. 2 is obtained from the approximation fitting function estimated from 10 input-specific activities, *S(t)*, including our chosen value, *S(0)*, of 16.33 dpm $(gC)^{-1}$ in 1750 and the 9 input *S(t)* values in 2004 through 2012. The equations listed at the bottom of Table 1 are used in sequence in the table to calculate the 9 input-specific activities, *S(t)*. The approximation fitting function is used to estimate the annual mean expected specific activities, <*S(t)*>, in 1750 through 2018 for the Niwot Ridge site. Naturally, the lack of data points between 1750 and 2004 makes the exact shape of the curve uncertain in this interval. Parameter values are chosen so that the <*S(t)*> values yield a fit that does not deviate significantly from the points for the input *S(t)* values, most importantly the value of 14.87 dpm $(gC)^{-1}$ for *S(t)* in 2004 and our chosen *S(0)* value of 16.33 dpm $(gC)^{-1}$ in 1750. Parameter values, however, have been chosen so that the 10 points for the *S(t)* values and the solid line for the expected <*S(t)*> values in the figure provide a realistic representation of the initial small decreases and later more significant decreases in the specific activities expected after the start of the industrial revolution in 1750 and the increased burning of fossil fuels each year. The *S(t)* value of 14.05 dpm $(gC)^{-1}$ for 2018, based on extrapolated values of *D14C* and *d13C*, is 0.09 dpm $(gC)^{-1}$ more than the expected <*S(t)*> value of 13.96 dpm $(gC)^{-1}$ in 2018.

Methodology used to calculate $C_F(t)$ and $C_{NF}(t)$

The methodology used to calculate $C_F(t)$ and $C_{NF}(t)$ relies on two accepted facts: (1) the initial total mole fraction *C(0)* of (280 ± 10) ppm before 1750 has been essentially constant for several thousand years (Prentice et al. 2018) and (2) the production rate of ^{14}C atoms in the atmosphere has been essentially constant for at least 15,000 years (Eisenbud 1997). Therefore, the steady-state activity of ^{14}C per unit volume of the atmosphere also would have been constant except for the redistribution of CO_2 in the atmosphere in each year with its exchange reservoirs. The product *C(t) S(t)* is proportional to the activity per unit volume of the atmosphere, which varies each year depending on whether there is a net input or output, $DC_{NF}(t)$, of non-anthropogenic fossil CO_2 in the atmosphere. The change in the product, $DC_{NF}(t)\ S(t)$, each year is independent of the value of $C_F(t)$ in the atmosphere because it contains no activity of ^{14}C. Also, except for the dilution of *S(0)* by the anthropogenic fossil component, *C(t)*, present in the atmosphere each year, the ^{14}C specific activity, *S(t)*, would have remained constant at our chosen initial value, *S(0)*, of 16.33 dpm $(gC)^{-1}$ in 1750. This dilution effect is noted as the Suess effect (Suess 1967)[8].

[8]Wikipedia. https://en.wikipedia.org/wiki/Suess_effect. Accessed 12 October 2021.

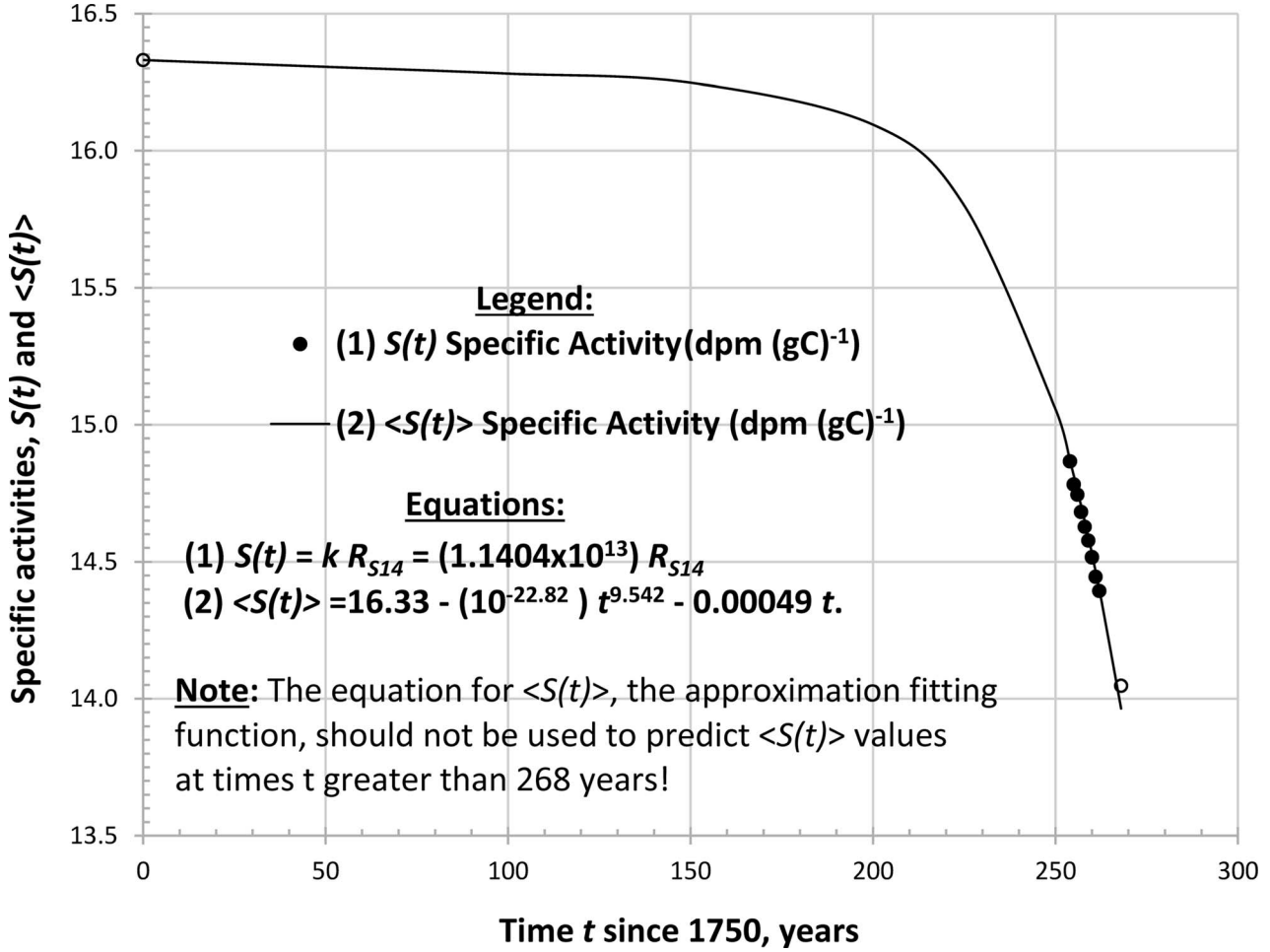

Fig. 2. Niwot Ridge, Colorado annual mean specific activity, *S(t)*, and expected specific activity,<*S(t)*>, of ^{14}C in *C(t)* in 1750 through 2018.

The value for the initial specific activity, *S(0)*, of 16.33 dpm $(gC)^{-1}$ is based upon the following information in the literature. For the average cosmogenic production rate of ^{14}C, we have adopted a value of 2.15 atoms cm^{-2} s^{-1}, based upon the average of the range limits of 1.8 and 2.5 atoms cm^{-2} s^{-1} (Mak et al. 1999) cited by Taylor et al. (2014). Additionally, we have used the value of 7.9 gC cm^{-2} for the areal density of carbon at Earth's surface, which considers contributions from the atmosphere, terrestrial biosphere, terrestrial humus, marine biosphere, and inorganic ocean carbon (Craig 1957). The quotient of the ^{14}C atom production rate of 2.15 atoms cm^{-2} s^{-1} by the areal density of 7.9 gC cm^{-3} yields our estimate of the steady state value for the specific activity *S(0)* of 0.2722 dps $(gC)^{-1}$ or 16.33 dpm $(gC)^{-1}$. The product, *C(0)S(0)K*, of respectively 280 ppm, 16.33 dpm $(gC)^{-1}$, and the constant *K* of 4.996×10^{-4} in units of gC m^{-3} $(ppm)^{-1}$ for NTP conditions, yields 2.284 dpm m^{-3} for *S(0)* in 1750. Our chosen value of 16.33 dpm $(gC)^{-1}$ for *S(0)* is larger than the value of 13.41 dpm $(gC)^{-1}$ for the 1950 standard and somewhat larger than values reported in the literature for ^{14}C dating.

Derivation of equations for the components of CO_2

In the derivation of equations for all components of CO_2 and their changes since 1750, the annual mean total CO_2 concentrations, *C(t)*, along with their ^{14}C specific activities, *S(t)*, are compared to the initial value, *C(0)*, and its specific activity, *S(0)*, present in 1750. Two logic pathways can be used to derive equations for $DC_{NF}(t)$, $C_{NF}(t)$, and $C_F(t)$:

Pathway 1: The statement for the change, $K\,DC_{NF}(t)\,S(t)$, of the ^{14}C activity per unit volume of the atmosphere at time *t* is: $K\,DC_{NF}(t)\,S(t) = K\,C(t)\,S(t) - K\,C(0)\,S(0)$, which yields:

$$DC_{NF}(t) = [C(t)\,S(t) - C(0)\,S(0)]\,S(t)^{-1} \rightarrow$$
$$C_{NF}(t) = C(0) + DC_{NF}(t) \rightarrow$$
$$C_F(t) = C(t) - C_{NF}(t).$$

Pathway 2: The equation for $DC_{NF}(t)$ above gives an expression for the specific activity, *S(t)*:

$$S(t) = C(0)\,S(0)\,[\,C(t) - DC_{NF}(t)]^{-1},$$

which reduces to the fundamental equation representing the specific activity, *S(t)* in *C(t)*, due to the dilution of *S(0)* in *C(0)* by the presence of $C_F(t)$ in *C(t)*:

$$S(t) = C(0)\,S(0)\,[\,C(t) - DC_{NF}(t)]^{-1}$$
$$= C(0)\,S(0)\,[\,(C_F(t) + C_{NF}(t)) - (C_{NF}(t) - C(0))]^{-1};\ \text{thus,}$$
$$S(t) = C(0)\,S(0)\,[C(0) + C_F(t)]^{-1}.$$

This fundamental equation for *S(t)*, based on the Suess effect, yields alternative equations for $C_F(t)$, $C_{NF}(t)$, and $DC_{NF}(t)$:

$$C_F(t) = \left[\left(S(0)S(t)^{-1} - 1\right]C(0) \rightarrow$$

$$C_{NF}(t) = C(t) - C_F(t) \rightarrow$$

$$DC_{NF}(t) = C_{NF}(t) - C(0).$$

A limited number of *D14C* values in 1750 through 2018 are available from NOAA for calculating the specific activities, *S(t)*. Values for expected specific activities, $\langle S(t)\rangle$ in 1750 through 2018, are estimated in Table 1 from eqn 2, the approximation fitting function described previously. When $\langle S(t)\rangle$ is substituted for *S(t)* for pathway 2 above, the equations are:

$$\langle C_F(t)\rangle = \left[S(0)\ \langle S(t)\rangle^{-1} - 1\right]C(0) \rightarrow$$

$$C_{NF}(t) = C(t) - \langle C_F(t)\rangle \rightarrow$$

$$DC_{NF}(t) = C_{NF}(t) - C(0),$$

where the value for the anthropogenic fossil component now is its expected value, $\langle C_F(t)\rangle$. These equations are used in Table 2 to calculate $\langle C_F(t)\rangle$, $C_{NF}(t)$, and $DC_{NF}(t)$, and they are displayed in Fig. 3 and Fig. 4. The equation for $\langle C_F(t)\rangle$ is independent of $DC_{NF}(t)$ and $C(t)$, and $\langle C_F(t)\rangle$ only varies over time t with the expected specific activity, $\langle S(t)\rangle$, in $C(t)$. It is noted that the equation for $\langle C_F(t)\rangle$ yields smaller values if smaller values of either *C(0)* or *S(0)* are selected.

RESULTS

The number of digits shown for quantities in cells of the tables often are less than those present; therefore, the reader will not be able to verify all listed quantities. The approximation fitting function listed below Table 1 is used to calculate the expected specific activities, $\langle S(t)\rangle$ in $C(t)$, listed in Table 2 and in Table 2a. Values of $\langle S(t)\rangle$ and $C(t)$ are used in Table 2 and Table 2a in calculating the expected anthropogenic fossil component, $\langle C_F(t)\rangle$, which then is used along with the total CO_2 concentration, $C(t)$, to

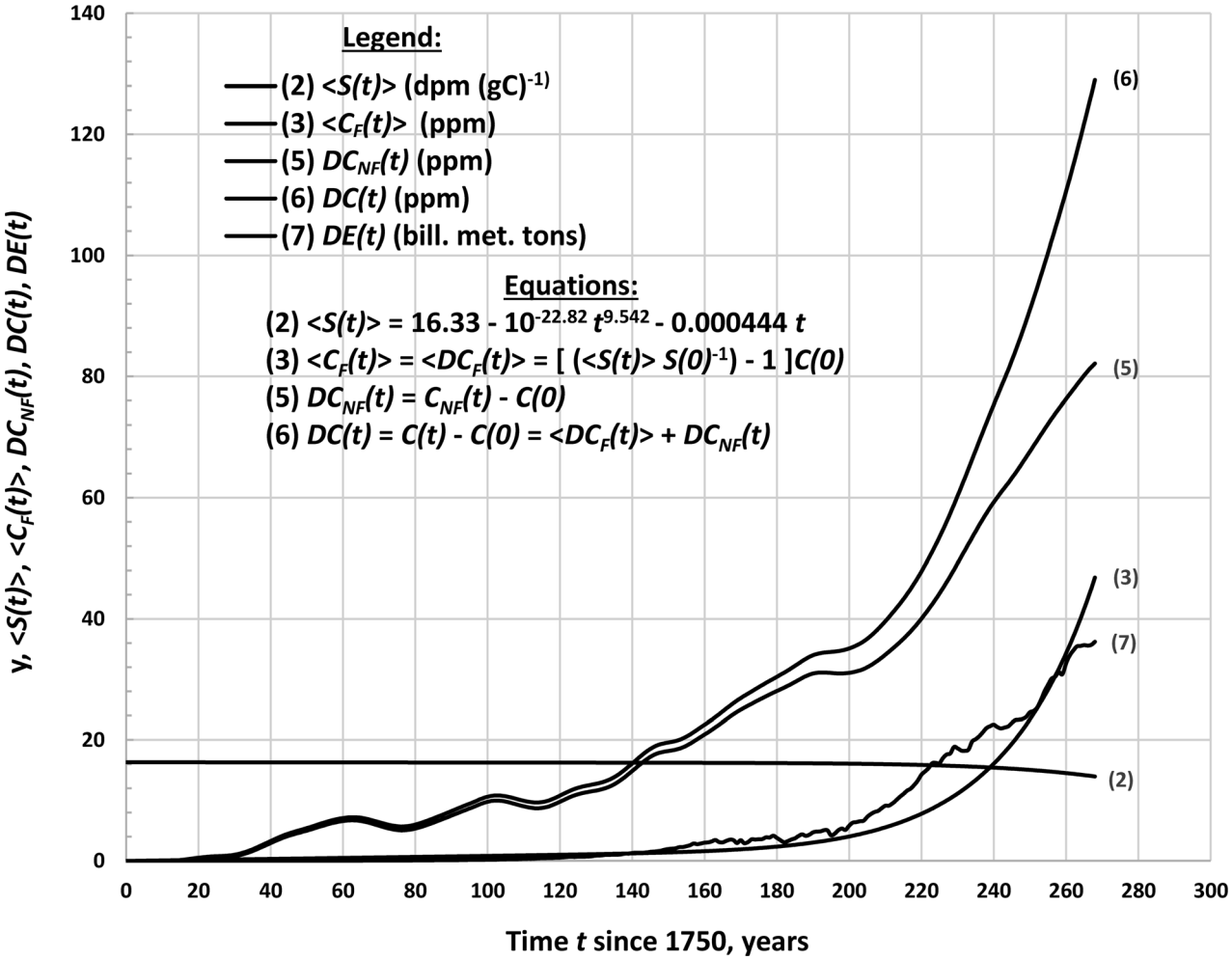

Fig. 3. *DC(t)*, $\langle S(t)\rangle$, $\langle C_F(t)\rangle$, $DC_{NF}(t)$, and *DE(t)* vs. time *t*.

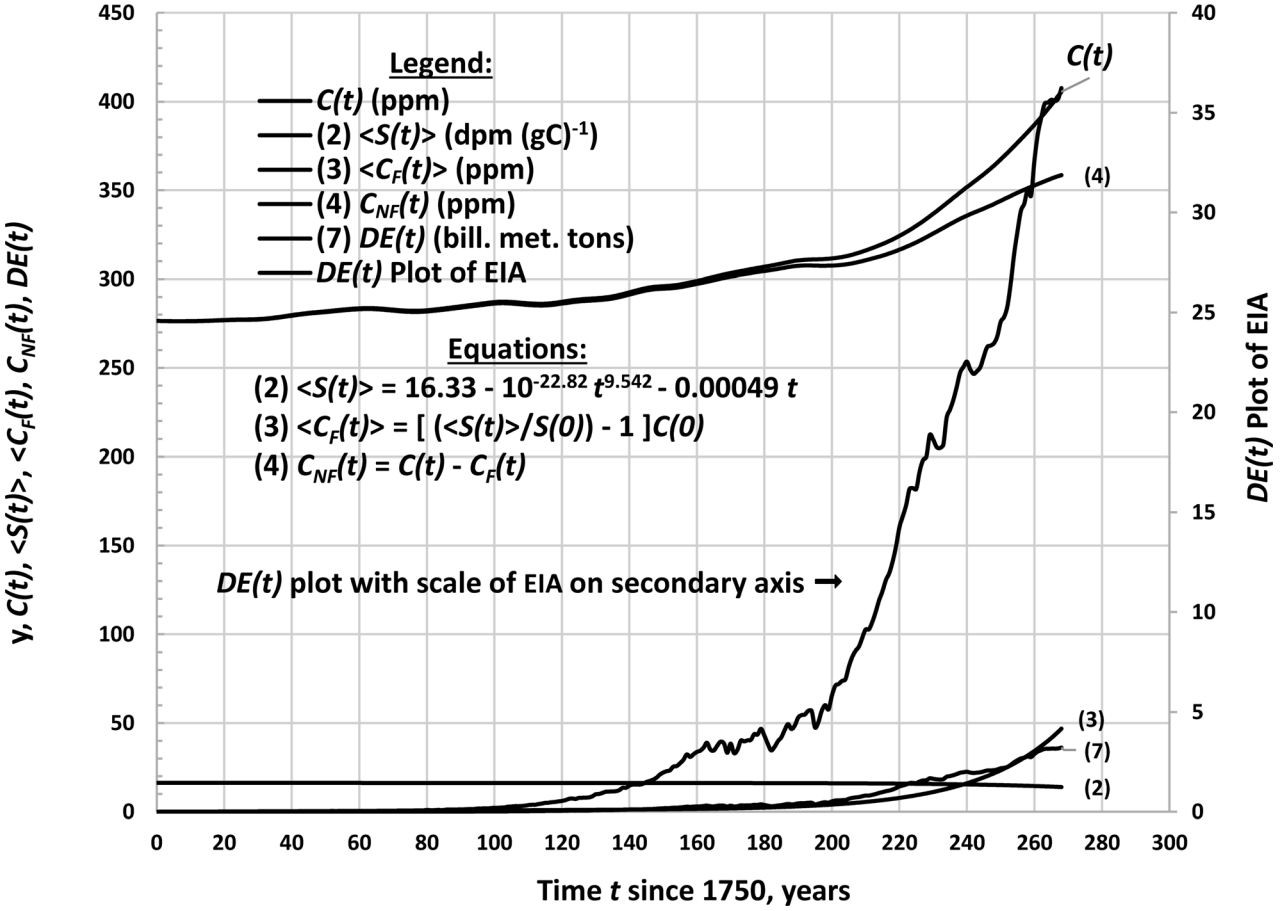

Fig. 4. $C(t)$, $\langle S(t)\rangle$, $\langle C_F(t)\rangle$, $C_{NF}(t)$ and $DE(t)$ vs. time t.

calculate the non-fossil component, $C_{NF}(t)$, and other CO_2 quantities listed in the tables and plotted in Fig. 3 through Fig. 5.

DISCUSSION

Discussion of results in Table 1 and Fig. 2

The primary purpose of Table 1 and Fig. 2 is the estimation of the expected specific activities, $\langle S(t)\rangle$, listed in Table 2 (http://links.lww.com/HP/A210) and Table 2a, but other unrelated results are provided and discussed here because of their relevance to the primary results and conclusions. The content of Table 1 and Fig. 2 has been discussed in Results and other sections above. Relative % changes in all CO_2 quantities in 2004 to those in 2018 are listed below Table 2a.

The *D14C* value of 4.734‰ in Table 1 for 2018 is calculated from a linear fit to the values in 2004 through 2012: $D14C = -4.2148\ t + 1134.3$; $R^2 = 0.9969$.

The *d13C* value of −8.573‰ in Table 1 for 2018 is an extrapolated value calculated from a linear fit to the values in 2004 through 2014:

$$d13C = -0.026\ t - 1.6052;\ R^2 = 0.9648.$$

The ratio of the slope in the equation for *D14C* to that in the equation for *d13C* is 162, which represents the relative sensitivity of the *D14C* statistic to that of the *d13C* statistic for detecting increases in the anthropogenic fossil component from one year to the next.

Relative % changes listed below Table 1 are discussed as follows.

- The *D14* statistic has the largest relative change of −92.67%. This value reflects the excellent sensitivity of *D14C* for detecting changes from one year to the next, including those of the anthropogenic fossil component, $\langle C_F(t)\rangle$, which is reflected by the −5.51% change in the values of R_{S14} and $S(t)$ and by the −6.07% change in the $\langle S(t)\rangle$ value calculated from the approximation fitting function.
- The discrepancy of 0.56% between the % changes for the $S(t)$ and $\langle S(t)\rangle$ values is due to the discrepancy of 0.09 dpm $(gC)^{-1}$ between the $S(t)$ and $\langle S(t)\rangle$ values in 2018. This discrepancy of 0.09 dpm $(gC)^{-1}$ is 0.64% of the $\langle S(t)\rangle$ value of 13.96 dpm $(gC)^{-1}$.
- The largest difference between the $S(t)$ and $\langle S(t)\rangle$ values in 2004 to 2012 is 0.03 dpm $(gC)^{-1}$.

Table 2a. Partial world atmospheric CO_2, its ^{14}C specific activity, anthropogenic fossil and nonfossil components, and emissions (1750-2018).[a]

Year	Time t since 1750 (years)	$C(t)$ (ppm)	(2) $\langle S(t)\rangle$ (dpm $(gC)^{-1}$)	(3) $\langle C_F(t)\rangle$ (ppm)	(4) $C_{NF}(t)$ (ppm)	(5) $DC_{NF}(t)$ (ppm)	(6) $DC(t)$ (ppm)	(7) $DE(t)$ (bill. met. tons)
1750	**0**	**276.44**	**16.33**	**0.00**	**276.44**	**0.00**	**0.00**	**0.00**
1751	1	276.40	16.33	0.01	276.39	−0.05	−0.04	0.01
1800	50	281.86	16.31	0.42	281.44	5.00	5.42	0.03
1850	100	287.06	16.28	0.84	286.22	9.78	10.62	0.20
1900	150	296.03	16.25	1.40	294.63	18.19	19.59	1.96
1950	200	311.54	16.10	4.03	307.51	31.07	35.10	5.83
2000	250	367.43	15.06	23.39	344.04	67.60	90.99	24.53
2018	268	405.40	13.96	46.84	358.56	82.12	128.96	36.22

[a]Note: The sum of $DE(t)$ values each year through 2018 is 1.590×10^{18} g. In 2018, $\langle C_F(t)\rangle$ of 46.84 ppm present in the atmosphere corresponds to a total mass estimated as 3.664×10^{17} g or about 23% of the total emissions. Thus in 2018, 77% of the total emissions is in the atmosphere's exchange reservoirs (see text).

- The value of 16.33 dpm $(gC)^{-1}$ for our chosen value of $S(0)$ is the same as the expected value $\langle S(0)\rangle$.
- The *d13C* statistic has a relative change from 2004 to 2018 of 2.70%, which is much more than the −0.02% change in R_{S13}.
- All listed R_{S13} values in 2004 through 2018 are 0.01114. This value is not much different from the value of 0.01116 in 1750 calculated from the *d13C* value of −6.50‰ (Rubino et al. 2013).

Discussion of results in Table 2, Table 2a, and Fig. 3 through Fig. 5

Table 2 (http://links.lww.com/HP/A210) contains a listing of all the same quantities as those in Table 2a. Each

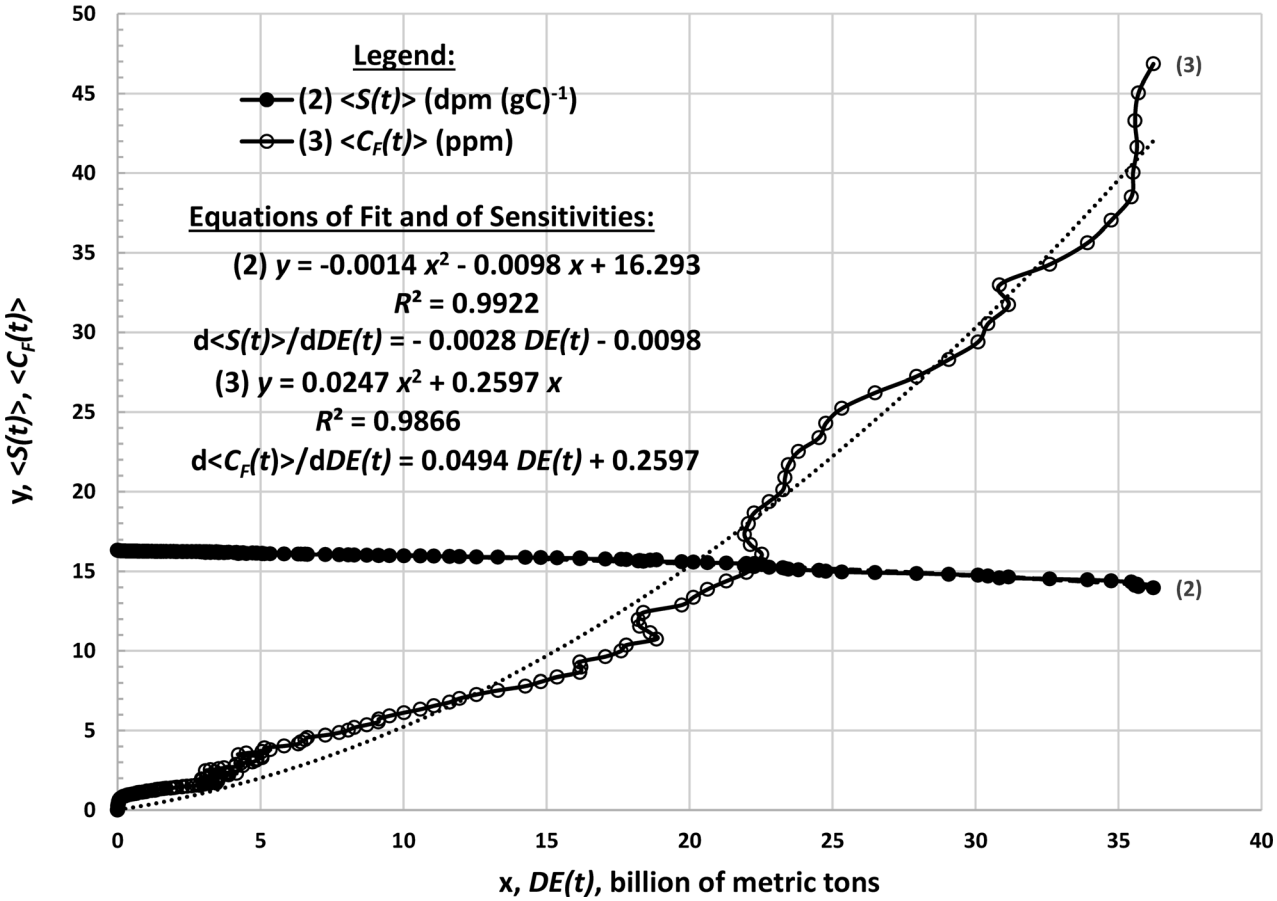

Fig. 5. $\langle S(t)\rangle$ and $\langle C_F(t)\rangle$ versus $DE(t)$.

table contains a listing of seven annual mean CO_2 quantities in 1750 through 2018. The symbol *C(t)* and the numbers (2) through (7) heading other columns are used as labels for the plots of all CO_2 quantities in Figs. 3, 4, and 5. The plot for *C(t)* is labeled as such. The numbers are placed before the symbols in legends, equations, and at the end of a line for a plot in each figure. Equations listed in the figures are used to calculate the quantities listed in columns (2) through (6) of each table. It is important to recognize in the following discussion that the value for $<C_F(t)>$ is identical to its annual change, $D<C_F(t)>$ since 1750 and that the sum of $D<C_F(t)>$, which is not specifically listed, and the annual change, $DC_{NF}(t)$, in the non-fossil component equals the annual change, *DC(t)*, in the total CO_2 concentration, *C(t)*.

Results in Table 2 are plotted in the figures versus the time *t* since 1750, and they are discussed along with plots in Figs. 3 as follows. In 1750 ($t = 0$), the initial value of 276.44 ppm listed for both *C(0)* and $C_{NF}(0)$ in Table 2a has been estimated from the Table 2 values of *C(t)* in 1751 and in 1752 of, respectively, 276.40 ppm and 276.36 ppm. Except for these values and the initial *S(0)* value of 16.33 dpm $(gC)^{-1}$, the initial values of other quantities are assumed to be zero. In 1751, a value of 0.01 ppm is listed for $C_F(t)$, and slightly negative values of −0.05 ppm and of −0.04 ppm are listed respectively for $DC_{NF}(t)$ and *DC(t)* in Table 2 and Table 2a, both of which do not become positive until 1765 and thereafter. These negative values may be associated with the Little Ice Age[9] when temperatures and CO_2 concentrations coincidentally had their lowest values in about 1750. Values for the anthropogenic fossil component, $<C_F(t)>$, in Table 2a and in plot 3 of Fig. 3 slowly increase from 0.01 ppm in 1751 to a value of 4.03 ppm in 1950. This $<C_F(t)>$ value of 4.03 ppm is 13.0% of the $DC_{NF}(t)$ value of 31.07 ppm and 11.5% of the *DC(t)* value of 35.10 ppm, which equals the sum of $<C_F(t)>$ and $DC_{NF}(t)$. After 1950, values of $<C_F(t)>$, $DC_{NF}(t)$, and *DC(t)* in Fig. 3 begin to increase rapidly. The increase in $<C_F(t)>$ coincides with the rapid increase after 1950 in the values of the annual emissions, *DE(t)*, of anthropogenic fossil CO_2 in Table 2 and Table 2a as well as in plot (7) in Fig. 3. Coincidentally, for the scale used on the primary vertical axis, the values for plot (3) of $<C_F(t)>$ and the plot (7) of *DE(t)* overlap until about 1900. The values in plot (5) of $DC_{NF}(t)$ and in plot (6) of *DC(t)* overlap each other early on, and then their plots slowly separate until 1950. After 1950, plots of both quantities increase more rapidly and their separation becomes greater each year. This separation is the value of $<C_F(t)>$. In Table 2a in 2018, $<C_F(t)>$ is 46.84 ppm and $DC_{NF}(t)$ is 82.12 ppm. Their sum of 128.96 ppm equals the value of *DC(t)*.

[9]Wikipedia. https://en.wikipedia.org/wiki/Little_Ice_Age. Accessed 12 October 2021.

The following discussion applies to quantities plotted in Fig. 4. The total CO_2 concentration, *C(t)*, equals the sum of the value in plot (4) for $C_{NF}(t)$ and in plot (3) for $<C_F(t)>$. Values in plot (2) are for the expected specific activity of ^{14}C, $<S(t)>$. Equations used for calculating $<S(t)>$, $<C_F(t)>$, and $C_{NF}(t)$ are listed in the figure. Two plots are provided for the annual CO_2 emissions reported by the Environmental Information Agency (EIA 2020) listed in Table 2 (Table SDC 1, http://links.lww.com/HP/A210) and designated here as *DE(t)*. Plot 7 for *DE(t)* uses the scale of the primary vertical axis on the left in Fig. 4. The unnumbered plot designated as "*DE(t)* plot with scale of EIA on secondary axis" uses the scale on the right. This same scale is used for the EIA plot of "CO_2 emissions" in the figure provided in the EIA reference. Consequently, the plot of *DE(t)* values using the scale of the secondary vertical axis appear here to be $450(40)^{-1}$ or 11.5 times the values in plot 7. Also, the slopes of the *DE(t)* plot of EIA at each time *t* are 11.5 times those in plot (7). Absent plot (4) for $C_{NF}(t)$ and plot (3) for $<C_F(t)>$, one might falsely conclude that the increase in the total CO_2 concentration, *C(t)*, in its plot after 1950 ($t = 200$ y) is due entirely to the increase in the anthropogenic fossil component, $C_F(t)$.

The following discussion applies to quantities plotted in Fig. 5. Displayed in the figure are plot (2) of $<S(t)>$ and plot (3) of $<C_F(t)>$ versus *DE(t)*; equations for their second order polynomial fits including R^2 values; and points for their annual mean values in 1750 through 2018. The *y* intercept in plot 2 of *S(t)* is 16.293 dpm $(gC)^{-1}$, which is slightly less than the $<S(0)>$ value of 16.33 dpm $(gC)^{-1}$ listed in Table 2a. The *y* intercept in plot 3 of $<C(t)>$ is zero. The sensitivities are the slopes of the plots of each quantity, and they represent their changes per unit of *DE(t)* of 1 billion metric tons. These are estimated by the equations displayed for the rates of change of $<S(t)>$ and $<C_F(t)>$ with respect to *DE(t)*. Both the magnitude and slope of the plot for $<S(t)>$ decrease very little, while those for the plot of $<C_F(t)>$ increase much more over the entire range of *DE(t)* from 0 in 1750 to 36.22 billion metric tons in 2018.

Anthropogenic fossil CO_2 in 2018 relative to the total of its annual emissions

The Table 2a value of the atmospheric concentration, $<C_F(t)>$, of anthropogenic fossil derived CO_2 in 2018 is 46.84 ppm. It is assumed that $<C_F(t)>$ is representative of its molar concentration throughout the entire atmosphere and that the total mass of the atmosphere is 5.148×10^{18} kg (Trenberth and Smith 2005) with an effective molecular weight of 28.96 g $mole^{-1}$. The number of moles, N_F, of anthropogenic fossil CO_2 present in the atmosphere then is calculated:

$$N_F = \left(46.84 \times 10^{-6}\right)\left(5.148 \times 10^{21}\,\mathrm{g}\right)\left(28.96\ \mathrm{g\,mole^{-1}}\right)^{-1}$$
$$= 8.326 \times 10^{15}\ \text{moles}.$$

Based on a molecular weight of 44.01 g mole^{-1} for CO, the total mass of anthropogenic fossil CO_2 present in the atmosphere in 2018 is calculated as 3.664×10^{17} g. The Table 2 value of 1,589.86 billion metric tons of anthropogenic fossil-derived CO_2 emitted into the atmosphere in 1751 through 2018 (EIA 2020a and 2020b) represents 1.590×10^{18} g. The inference is that the quantity of anthropogenic fossil CO_2 in the atmosphere in 2018 represents about 23% of the total amount of anthropogenic fossil-derived CO_2 that had been released to the atmosphere since 1750.

Therefore, 77% of the total anthropogenic fossil emissions of CO_2 then would be present in the atmosphere's exchange reservoirs in 2018. These results differ significantly from those reported by others: "Using these data, Keeling was able to compare the amount of CO_2 accumulating in the atmosphere against estimates of the amount of CO_2 being released by burning fossil fuels. The atmospheric fraction appeared to be approximately 55%, meaning that roughly half of all CO_2 released by coal, oil, and natural gas was remaining in the atmosphere, thus causing the Keeling Curve's annual rise" (Harris 2010).

Values of *$S(t)$ and *$D14C$ statistics required to support claims of the dominance of $C_F(t)$

Larger reductions in values for the annual mean $\langle S(t) \rangle$ and $D14C$ statistics are required to support claims that the increase, $DC(t)$, in 2018 (t = 268 y) above $C(0)$ in 1750 (t = 0) has been dominated by or is equal to the anthropogenic fossil component, $C_F(t)$, in 2018. Quantities of CO_2 in 1750 and 2018 are as follows. Table 2a includes $C(0)$ of 276.44 ppm; $S(0)$ of 16.33 dpm (gC)$^{-1}$; $C(t)$ of 405.40 ppm; $DC(t)$ of 128.96 ppm; $\langle S(t) \rangle$ of 13.96 dpm (gC)$^{-1}$; and $\langle C_F(t) \rangle$ of 46.84 ppm, which is a fraction F of 0.3632 of $DC(t)$. Table 1 includes in 2018: $D14C$ of 4.734‰; F_d of 0.9918; F_{13} of 0.9671; and S_{std14} of 13.41 dpm (gC)$^{-1}$. The equation for the specific activity based on the Suess effect is expressed: $S(t) = S(0)\,[1 + CF(t)C(0)^{-1}]^{-1}$. Equations for calculating *$S(t)$ and *$D14C$ values required for $C_F(t)$ in 2018 to equal a given fraction, F, of $DC(t)$ are expressed:

$$*S(t) = \frac{S(0)}{1 + \left(\frac{FDC(t)}{C(0)}\right)}, \textit{whose value gives:}$$

$$*D14C = \left(\frac{*S(t)F_dF_{13}}{S_{std14}} - 1\right)1,000‰$$

To achieve an F value of 0.5, *$S(t)$ would have to be 13.24 dpm (gC)$^{-1}$ instead of 13.96 dpm (gC)$^{-1}$, and *$D14C$ would have to be −52.89‰ instead of 4.734‰. Also $C_F(t)$, $DC_{NF}(t)$, and $C_{NF}(t)$ would have values, respectively, of 64.48 ppm, 64.48 ppm, and 340.92 ppm. To achieve an F value of 1, *$S(t)$ would have to be 11.14 dpm (gC)$^{-1}$ instead of 13.96 dpm (gC)$^{-1}$, and *$D14C$ would have to be −203.5‰ instead of 4.734‰. Also, $C_F(t)$ would have the value of $DC(t)$ of 128.96 ppm, $DC_{NF}(t)$ the value of 0, and $C_{NF}(t)$ the value of $C(0)$ of 276.44 ppm. These results, especially those for $D14C$, negate the claims that all or most of the increase of CO_2 since 1750 has been due to the burning of fossil fuel.

CONCLUSION

Results in this paper and citations in the scientific literature support the following 10 conclusions.

1. The scientific literature does not appear to provide estimates of either the annual mean values of the anthropogenic fossil component, $C_F(t)$, or of the non-fossil component, $C_{NF}(t)$, present in the total atmospheric CO_2 concentration, $C(t)$, nor their respective changes from values in 1750.
2. The annual mean values of all CO_2 quantities provided in this paper automatically account for the redistribution of CO_2 among its reservoirs, including all of its isotopic forms. Results depend on chosen values in 1750 of 276.44 ppm for $C(0)$ and 16.33 dpm (gC)$^{-1}$ for $S(0)$, both of which may be somewhat overestimated as indicated in the text. Based on the simple equations used to calculate all CO_2 quantities, smaller values for these chosen quantities would yield smaller values of the anthropogenic fossil component, $C_F(t)$, and larger values of the non-fossil component, $C_{NF}(t)$.
3. In 1950, the $\langle C_F(t) \rangle$ value of 4.03 ppm in Table 2a is 1.29 % of $C(t)$ and 11.48% of the increase, $DC(t)$, of 35.10 ppm since 1750. After 1950, values of the two components of $C(t)$ begin to increase rapidly, and this increase continues through 2018. This rapid increase, however, is not triggered by the greenhouse effect and global warming associated with either the 1950 value of 4.03 ppm for $C_F(t)$ or the relatively small increase in the annual change, $DC_{NF}(t)$, of 31.07 ppm in the non-fossil component, which is 88.5% of the $DC(t)$ value of 35.10 ppm. This $DC_{NF}(t)$ value of 31.07 ppm in 1950 results from the annual redistribution of CO_2 among its reservoirs, primarily a net release of CO_2 from the oceans due to increases in temperatures from solar insolation in 1950 and afterwards.
4. In 2018, the $\langle C_F(t) \rangle$ value of 46.84 ppm is 11.55% of the $C(t)$ value of 405.40 ppm, 36.32% of the $DC(t)$ value of 128.96 ppm, and 57.04% of the $DC_{NF}(t)$ value of 82.12 ppm. These results negate claims that the increase, $DC(t)$, in $C(t)$, since 1750 has been dominated by the increase of the anthropogenic fossil component, $C_F(t)$.
5. In 2018, the total content of anthropogenic fossil CO_2 in the atmosphere is estimated as 3.664×10^{17} g, which is 23% of the total emissions of 1.590×10^{18} g since 1750. Thus, in 2018, 77% of the total emissions is estimated to be present in the atmosphere's exchange reservoirs.

6. Claims of the dominance of the anthropogenic component, $C_F(t)$, in the increase of the CO_2 concentration, $C(t)$, first began in 1960 with: "Keeling Curve: Increase in CO_2 from burning fossil fuel" (Rubino 2013). Despite the lack of knowledge of the two components of $C(t)$, these claims have continued in the scientific literature.
7. Calculated much larger reductions in values for the annual mean *D14C* statistic and other reductions in the $<S(t)>$ statistic in Table 1 are required to support the claims that the increase of the total concentration, $C(t)$ above $C(0)$ in 1750 has been dominated by or is equal to the increase in the anthropogenic fossil component, $C_F(t)$. These results negate the claims of the dominance of $C_F(t)$ in the increase of $C(t)$.
8. Claims of the dominance of the anthropogenic fossil component have involved (a) the misuse of the *d13C* and *D14C* statistics to validate these claims when they are expressed in the common unit of per mil (‰), which causes their slopes in plots to be magnified by a factor of 1,000 above what they otherwise would be; (b) the plot of decreasing values of the *d13C* statistic along with the plot of increasing values of the total CO_2 concentration, $C(t)$, in the same figure on different vertical axes to infer or claim that the increase in $C(t)$ is due mostly or entirely to the anthropogenic fossil component, $C_F(t)$, even though large reductions of the *d13C* statistic reflect no significant changes in its ($^{13}C/^{12}C$) atom ratios and bear no significant relationship with increases in the anthropogenic fossil component, $C_F(t)$; and (c) EIA plot of the CO_2 concentration, $C(t)$, in the same figure with the plot of the annual emissions, $DE(t)$, of anthropogenic fossil-derived CO_2 on different vertical scales, which provides the inference that the anthropogenic fossil component, $C_F(t)$, is responsible for the increase in $C(t)$ when a plot of the non-fossil component, $C_{NF}(t)$, and of the anthropogenic fossil component, $C_F(t)$, are not included in the EIA figure.
9. An article on Glacial-Interglacial Cycles (NOAA) suggests that recent increases in CO_2 and temperatures are due primarily to cyclic changes of solar radiation associated with Earth's orbit about the sun. The annual change, $DC_{NF}(t)$, in the non-fossil component has positive increasing values in Table 2 (http://links.lww.com/HP/A210) after 1764. It will eventually become negative in the next glacial period when average temperatures decrease again as they have done over all of the previous glacial-interglacial cycles.
10. The assumption that the increase in CO_2 since 1800 is dominated by or equal to the increase in the anthropogenic component is not settled science. Unsupported conclusions of the dominance of the anthropogenic fossil component of CO_2 and concerns of its effect on climate change and global warming have severe potential societal implications that press the need for very costly remedial actions that may be misdirected, presently unnecessary, and ineffective in curbing global warming.

Acknowledgments—This paper is dedicated to the memory of our colleague, Dr. Michael T. Ryan, past Editor-in-Chief of *Health Physics*, and to Dr. Mary Gene Ryan, Managing Editor, who provided us with guidance and encouragement in the submission of our paper.

REFERENCES

CSIRO. Report, State of the Climate 2014. Australian Government, Bureau of Meteorology and the Commonwealth Scientific and Industrial Research Organization (CSIRO) [online]. 2014. Available at ***http://www.bom.gov.au/state-of-the-climate/2014/***. Accessed 26 October 2021.

Craig H. The natural distribution of radiocarbon and the exchange time of carbon dioxide between the atmosphere and sea. Tellus 9:1–17; 1957.

EIA. U.S. Energy Information Administration. World carbon dioxide (CO_2) emissions from fossil fuel combustion and global atmospheric concentrations CO_2 (1751-2018). Oak Ridge, TN: ORNL; Oak Ridge National Laboratory, Carbon Dioxide Information Analysis Center, Scripps Institute of Oceanography CO_2 program; U.S. Energy Information Administration, International Energy Statistics [online]. 2020a. Available at ***https://www.eia.gov/energyexplained/energy-and-the-environment/greenhouse-gases-and-the-climate.php***. Accessed 7 December 2020.

EIA. U.S. Energy Information Administration. Energy and the environment explained. Greenhouse gases and the climate [online]. 2020b. Available at ***https://www.eia.gov/energyexplained/energy-and-the-environment/greenhouse-gases-and-the-climate.php***. Accessed 7 December 2020.

Eisenbud M, Gesell T. Environmental radioactivity. New York: Academic Press; 1997.

Gerlach T. Volcanic versus anthropogenic carbon dioxide. EOS 92:201–208; 2011.

Harris DC. Charles David Keeling and the story of atmospheric CO_2 measurements. Anal Chem 82:7865–7870; 2010. Available at ***https://www.acs.org/content/acs/en/education/whatischemistry/landmarks/keeling-curve.html***. Accessed 26 October 2021.

Karlen I, Olsson IU, Kallburg P, Kilici S. Absolute determination of the activity of two ^{14}C dating standards. Arkiv Geofysik 4: 465–471; 1964.

Keeling CD. The concentration and isotopic abundances of carbon dioxide in the atmosphere. Tellus 12:200–203; 1960. Available at ***https://scrippsco2.ucsd.edu/history_legacy/early_keeling_curve.html***. Accessed 26 October 2021.

Lehman SJ, Miller JB 2019, University of Colorado, Institute of Alpine and Arctic Research (INSTAR), Radiocarbon Composition of Atmospheric Carbon Dioxide ($^{14}CO_2$) from the NOAA ESRL Carbon Cycle Cooperative Global Air Sampling Network, 2003-2018, Version: 2019-07-15, 2019: AND

Lehman SJ, Miller JB, Wolak C, Southon J, Tans PP, Montzka SA, Sweeney C, Andrews A, LaFranchi B, Guilderson TP, Turnbull JC. Allocation of Terrestrial Carbon Sources Using $^{14}CO_2$: Methods, Measurement, and Modeling. Radiocarbon 55,1484–1495; 2013. 10.1017/S0033822200048414, 2013.

Mak J, Brenninkmeijer C, Southon J. Direct measurement of the production rate of C-14 near Earth's surface. Geophys Res Lett 26:3381–3384; 1999.

Miller JB, Lehman S, Wolak C, Turnbull J, Dunn G, Graven H, Keeling R, Meijer HAJ, Aerts-Bijma AT, Palstra SWL, Smith AM, Allison C, Southon J, Xu X, Nakazawa T, Aoki S, Nakamura T, Guilderson T, LaFranchi B, Mukai H, Terao Y, Uchida M, Kondo M. Initial results of an intercomparison of AMS-based atmospheric $^{14}CO_2$ measurements. Radiocarbon 55:1475–1483; 2013.

Prentice IC, Farquhar GD, Fasham MJR, Goulden ML, Heimann M, Jaramillo VJ, Kheshgi HS, Le Quéré C, Scholes RJ, Wallace DWR. The carbon cycle and atmospheric carbon dioxide [online]. 2018. Available at ***https://www.ipcc.ch/site/assets/uploads/2018/02/TAR-03.pdf***. Accessed 26 October 2021.

Rubino M, Etheridge DM, Trudinger CM, C. E. Allison, M. O. Battle, R. L. Langenfelds, L. P. Steele, M. Curran, M. Bender, J. W. C. White,T. M. Jenk,T. Blunier, R. J. FranceyA revised 1000 year atmospheric δ ^{13}C-CO_2 record from Law Dome and South Pole, Antarctica. J Geophys Res Atmos 118:8482–8499; 2013. Available at ***https://agupubs.onlinelibrary.wiley.com/doi/full/10.1002/jgrd.50668***. Accessed 26 October 2021.

Rubino M, Etheridge DM. Greenhouse gases in the atmosphere based on global observations through 2018 [online]. 2019. Available at ***https://library.wmo.int/doc_num.php?explnum_id=10100***. Accessed 26 October 2021.

Skrable K, Chabot G, French C. Table 2. World atmospheric CO_2, its C-14 specific activity, anthropogenic fossil component, non-fossil component, and emissions (1750-2018); 2021. Available at ***http://links.lww.com/HP/A210***.

Suess HE, Houtermans J, Munk W. The effect of industrial fuel combustion on the carbon-14 level of atmospheric CO_2. In: Proceedings of the Monaco Symposium on Radioactive Dating and Methods of Low-Level Counting. Vienna: IAEA; 1967: 57–68.

Taylor RE, Bar-Yosef, Ofer, Renfrew, Colin. Radiocarbon dating: an archaeological perspective. Foreword. Walnut Creek, CA: Left Coast Press; 2014.

Trenberth KE, Smith L. The mass of the atmosphere: a constraint on global analyses. J Climate 18:864–875; 2005.

Water Encyclopedia. Lehr JH, Keeley J, eds. Carbon dioxide in the ocean and atmosphere/natural ocean carbon cycle. Water encyclopedia [online]. 2005. Available at ***http://www.waterencyclopedia.com/Bi-Ca/Carbon-Dioxide-in-the-Ocean-and-Atmosphere.html***. Accessed 26 October 2021.

White JWC, Vaughn BH, Michel SE. University of Colorado, Institute of Arctic and Alpine Research (INSTAAR), stable isotopic composition of atmospheric carbon dioxide (^{13}C and ^{18}O) from the NOAA ESRL Carbon Cycle Cooperative Global Air Sampling Network, 1990-2014, Version: 2015-10-26. 2015.

■■

APPENDIX

Definitions of symbols, constants, and standards for CO_2 quantities are listed alphabetically as follows at time t years after 1750 along with initial values in 1750 and values for 1950 standards.

C(0) ≡ initial total concentration of atmospheric CO_2 in 1750 = 276.44 ppm.

C(t) ≡ total concentration of atmospheric CO_2 at time t, ppm.

$C_F(0)$ ≡ initial anthropogenic fossil component present in *C(0)* = 0.

$C_F(t)$ ≡ anthropogenic fossil component present in *C(t)* at time *t*, ppm.

$\langle C_F(t) \rangle$ ≡ expected anthropogenic fossil component present in *C(t)* at time *t*, ppm.

$C_{NF}(0)$ ≡ initial non-anthropogenic fossil component present in 1750 = *C(0)* = 276.44 ppm.

$C_{NF}(t)$ ≡ non-anthropogenic fossil component present in *C(t)* at time *t*, ppm.

DC(t) ≡ increase in *C(t)* above *C(0)*, ppm.

$DC_F(t)$ ≡ increase in $C_F(t)$ above $C_F(0) = C_F(t)$, ppm.

$\langle DC_F(t) \rangle$ ≡ expected increase in $C_F(t)$ above $C_F(0) = \langle C_F(t) \rangle$, ppm.

$DC_{NF}(t)$ ≡ increase in $C_{NF}(t)$ above $C_{NF}(0)$, ppm.

DE(0) ≡ initial annual emission of anthropogenic fossil component, $C_F(t)$, in 1750 = 0.

DE(t) ≡ annual emission of anthropogenic fossil component, $C_F(t)$, billions of metric tons.

d13C ≡ 1,000‰ times the deviation of the annual mean ratio, R_{S13}, of ($^{13}C/^{12}C$) atoms in *C(t)* from that of a 1950 standard, R_{std13}, relative to R_{std13}, ‰ = −6.5‰ in 1750. The *d13C* value of the 1950 standard = −25‰.

D14C ≡ 1,000‰ times the deviation of the annual mean ratio, R_{S14}, of ($^{14}C/^{12}C$) atoms in *C(t)* multiplied by factors, F_d and F_{13}, from that of a 1950 standard, R_{std14}, relative to R_{std14}, ‰.

**D14C* ≡ required value of *D14C* for anthropogenic fossil component, $C_F(t)$, to equal a given fraction *F* of the increase, *DC(t)*, of *C(t)*, from 1750 (*t* = 0) to 2018 (*t* = 268 y).

F_d ≡ factor in equation for *D14C* to account for the decay of ^{14}C atoms in the year of the annual mean value for *D14C* relative to that of the 1950 standard.

F_{13} ≡ factor in equation for *D14C* to account for the fractionation of ^{13}C atoms in the year of the annual mean value for *D14C* relative to that of the 1950 standard.

k ≡ constant of 1.404×10^{13} dpm $(gC)^{-1}$ per unit ($^{14}C/^{12}C$) ratio.

K ≡ constant of 4.996×10^{-4} gCm^{-3} /ppm for converting concentration of CO_2 in ppm to gC m^{-3} under NTP conditions.

R_{std13} ≡ ($^{13}C/^{12}C$) atom ratio of standard = 0.011237 in 1950.

R_{std14} ≡ ($^{14}C/^{12}C$) atom ratio of standard $=1.176 \times 10^{-12}$ in 1950.

S(t) ≡ annual mean specific activity of *C(t)*, dpm $(gC)^{-1}$.

**S(t)* ≡ required value of *S(t)* for anthropogenic fossil component, $C_F(t)$, to equal a given fraction *F* of the increase, *DC(t)*, from 1750 (*t* = 0) to 2018 (*t* = 268 y).

$\langle S(t) \rangle$ ≡ expected specific activity of *C(t)* calculated from eqn (2) for the approximation fitting function, dpm $(gC)^{-1}$.

t ≡ time in years from 1750 to the year of an annual mean value of a CO_2 quantity, for example, *t* equals 1 year in 1751 and 200 years in 1950, the year for the 1950 standard.